Parametric neutrino flavor conversions and Rabi oscillations

Lei Ma* and Huaiyu Duan†
Department of Physics & Astronomy, University of New Mexico, Albuquerque, NM 87131, USA

Shashank Shalgar‡
Theoretical Division, Los Alamos National Laboratory, Los Alamos, NM 87545, USA
(Dated: February 18, 2017)

We develop an interpretation of neutrino flavor conversions in fluctuating matter density based on Rabi oscillations. In certain limits, matter density fluctuations with single frequency modulates the neutrino flavor conversion similar to Rabi oscillations in optics. Adding more frequencies in matter fluctuations have complicated effects on the neutrino flavor conversions, which is interference between each frequencies. The interference is explored and criteria of interference is proposed and verified numerically. By switching to a new basis, we are able to expand neutrino flavor conversions in matter with multiple-frequency fluctuations into superposition of Rabi oscillations. Using this technique we explain the relation between neutrino flavor conversions and Rabi oscillations by taking into account of the interference between different modes of Rabi oscillations more quantitatively.

I. INTRODUCTION

In several astrophysical environments, such as core-collapse supernova, neutrinos propagate through dense fluctuating medium. The neutrinos experience a potential due forward scattering which dramatically modifies the flavor oscillation probability. Modification of neutrino flavor oscillations due medium played a vital role in the resolution of the Solar neutrino problem [1–3]. Varying matter density in the medium can lead to several interesting phenomenology, such as parametric resonance, as demonstrated in [4, 5].

As one of the most intense neutrino sources, supernova neutrinos experience turbulent matter density as they propagate out [6, 7]. The flavor conversion can be modified by forward scattering off turbulent matter in this scenario. The turbulent matter density environment for neutrino flavor conversion has been studied for a long time [8–10]. However, interest in this topic has been reawakened with a new approach to the topic based on Jacobi-Anger expansion by Kneller, et al. [11, 12]. The resurgence of interest in the topic also has to do with the realization that the neutrino flavor oscillations in the interior of a core-collapse supernova is not very well understood due to additional modification to neutrino flavor oscillations introduced by self-interactions(Lots of collective neutrino oscillation references). Whether, neutrino flavor oscillations play a role in modifying neutrino wind induced convection or R-process nucleosynthesis is an unsettled question. However, the lack of understanding of neutrino oscillations in the interior of a core-collapse supernova is a motivation to gain a better understanding of neutrino oscillations. In this paper we focus on a very narrow topic of neutrino flavor oscillations in turbulent matter with the hope that in the future it will help us gain a better understanding of neutrino flavor oscillations in the presence turbulence as well as neutrino self-interactions.

In this paper, we will first recapitulate the phenomenon of parametric resonance in the context of neutrino oscillations and interpret the matter stimulated neutrino flavor conversions [11, 12], as superposition of Rabi oscillations. **Explain the structure of the paper and the goal of the paper.**

II. BACKGROUND AND FORMALISM

In this section, we provide some background necessary for understanding of neutrino flavor oscillations in turbulent matter. We very briefly introduce the matter effect and as a precursor to neutrino flavor oscillations in turbulent medium, we discuss neutrino flavor oscillations in sinusoidally varying matter density. Throughout this paper we work in the two flavor approximation for sake of simplicity.

The neutrinos emitted in most astrophysical phenomenon are highly relativistic and hence the evolution of their wavefunction is governed by the Schrodinger equation,

$$i\frac{d}{dr}\Psi(r) \equiv i\frac{d}{dr}\begin{pmatrix}\psi_e(r)\\ \psi_\mu(r)\end{pmatrix} = H^f\begin{pmatrix}\psi_e(r)\\ \psi_\mu(r)\end{pmatrix}. \qquad (1)$$

Here, the Hamiltonian H^f is a 2×2 matrix and the superscript f denotes that the Hamiltonian is in the flavor basis. The physics of neutrino oscillations is obviously independent of the basis we choose but the form of the Hamiltonian is basis dependent. The basis in which the Hamiltonian is diagonal is defined as the mass basis. If the neutrino weak eigenstates were identical to the neutrino mass eigenstates the flavor the Hamiltonian is a diagonal matrix in both bases. But, numerous neutrino oscillation experiments have provided sufficient evidence

* leima@unm.edu
† duan@unm.edu
‡ shashank@lanl.gov

for neutrino mixing and non-degenerate neutrino masses, which implies that the Hamiltonian is not diagonal in the flavor basis. It is a standard convention to parametrize the Hamiltonian in the following form,

$$H_{\rm v}^f = \frac{1}{2}\begin{pmatrix} -\omega_{\rm v}\cos 2\theta_{\rm v} & \omega_{\rm v}\sin 2\theta_{\rm v} \\ \omega_{\rm v}\sin 2\theta_{\rm v} & \omega_{\rm v}\cos 2\theta_{\rm v}\end{pmatrix}. \tag{2}$$

We have used the subscript v to denote that this is the Hamiltonian in vacuum and that we have not included the effect of medium in this Hamiltonian. The Hamiltonian has been written in a form that is traceless as the trace of the Hamiltonian contributes to the overall phase and has no physical consequence. The frequency of neutrino flavor oscillations is determined by $\omega \equiv \delta m^2/2E$, where E is the energy of the neutrino, whereas the amplitude is determined by the mixing angle $\theta_{\rm v}$. Neutrino flavor oscillations have a maximum amplitude of unity when the ratio of diagonal element to the off-diagonal element vanishes. In the absence of any medium this condition is satisfied only for vacuum mixing angle of $\pi/4$.

In the presence of a medium, the neutrinos undergo forward scattering from electrons and nuclei, but the forward scattering of neutrinos off nuclei can only happen via neutral current interactions that is identical for all flavors and can be ignored as it only contributes to an unobservable overall phase. The forward scattering of neutrinos of electron by definition does not change the momentum of the neutrinos but does introduce an additional phase in electron neutrinos compared to other flavor of neutrinos. The introduction of additional phase due to the electrons can be accommodated in the Hamiltonian by adding a potential that is proportional to the electron number density. The Hamiltonian in the presence of electrons in the medium can be written in the flavor basis as follows,

$$H^f \equiv H_{\rm v}^f + H_{\rm m}^f = \tag{3}$$

Again we choose to write the matter Hamiltonian neglecting the unphysical trace of the Hamiltonian. It can be easily seen from eq. **??** that the presence of the additional potential modifies the neutrino flavor oscillation frequency, which is the same as the determinant of the Hamiltonian part from a factor of two which is a matter of convention. Also, the effective mixing angle is modified as seen from the modified ratio of diagonal and off-diagonal elements of the Hamiltonian. In fact, we can see that there is a value of $\lambda = \sqrt{2}G_F n_e$ for which the ratio of diagonal to off-diagonal element vanishes, which as mentioned before, is a condition for maximal neutrino flavor oscillation.

In presence of constant matter density it is possible to define a 'matter basis' in which the Hamiltonian H^f is diagonal. The eigenstates in the matter basis do not oscillate from one state to another by definition. The existence of a basis in which we can define eigenstates makes the calculation of neutrino flavor oscillation probabilities much simpler. Although, this can be easily done in the case of constant matter density such a basis cannot be defined for matter density that fluctuates or is turbulent. However, there are some cases for which such a basis is possible.

In particular, let us consider the following equation of motion,

$$i\frac{d}{dr}\begin{pmatrix}\nu_1^m \\ \nu_2^m\end{pmatrix} = \frac{1}{2}\begin{pmatrix} -\omega_m & Ae^{ikr} \\ Ae^{-ikr} & \omega_m\end{pmatrix}. \tag{4}$$

The Schrodinger equation in eq. 4 does not correspond to a matter profile. However, we will show that the solution of the equation can help us write the solution of physical matter profiles. In order to solve eq. 4, we define a new basis,

$$\begin{pmatrix}\nu_1^{m\prime} \\ \nu_2^{m\prime}\end{pmatrix} = \begin{pmatrix} e^{-i\frac{kr}{2}} & 0 \\ 0 & e^{i\frac{kr}{2}}\end{pmatrix}\begin{pmatrix}\nu_1^m \\ \nu_2^m\end{pmatrix} \tag{5}$$

In this new basis eq. 4 the Schordinger equation is in a form that is very simple and the condition for resonance can be guessed by inspection,

$$i\frac{d}{dr}\begin{pmatrix}\nu_1^{m\prime} \\ \nu_2^{m\prime}\end{pmatrix} = \begin{pmatrix} -(\omega_m - k) & A \\ A & (\omega_m - k)\end{pmatrix}\begin{pmatrix}\nu_1^{m\prime} \\ \nu_2^{m\prime}\end{pmatrix}. \tag{6}$$

It is clear, that the condition for resonance is $\omega_m = k$. The resonance maximally converts $\nu_1^{m\prime}$ to $\nu_2^{m\prime}$. It can be shown that this condition is equivlaent to a maximal conversion between flavor eigenstates (**not clear here more explainatinon needed**). It should be noted that the transformation eq. 5, helps us write the Schrodinger equation in a way that clearly shows us the condition for resosnance, as the form of the equation is analogous to the equations of motion for flavor eigenstates in constant matter density. However the condition of resonance is obviously independent of the basis we choose. Away from the resonance the amplitude drops rapidly.

The phenomenon of parametric resonance described in the previous paragraph is very familiar to us in the context of classical physics. The resonant amplification of the transition amplitude is a result of matching of the natural frequency of the system with the driving frequency. A classical system like a simple pendulum with frequency f oscillates with an increasingly larger amplitude if a driving force of frequency f is applied to it. Let us imagine however a simple pendulum with frequency f that is given a push during every alternate period; we still expect a resonant enhancement of the amplitude. In general there is not a single frequency that can cause a resonant enhancement of oscillations but an infinite number of frequencies that can cause resonant enhancement of oscillations for a system.

Throughout the paper, we exploit this fact argue that Hamiltonian for any matter profile can be approximated by a series in which each component has the form similar to the one given in eq. **??**. We find that in many cases the number of terms that need to be maintained in the series is quite small ($\lesssim 10$). We also provide a systimatic criteria for deciding which terms should be included in the series and which terms are unimportant.

III. SINGLE FREQUENCY PROFILE

In this section, we look at the neutrino flavor oscillations in a medium that is a constant matter density plus a single frequency perturbation,

$$\lambda(r) = \lambda_0 + \delta\lambda(r) = \lambda_0 + A\cos(kr) \tag{7}$$

In absence of the sinusoidal pertubation the Hamiltonian can be written as a diagonal matrix in the matter basis. In this basis addition pertubation leads to an additional term for the Hamiltonian, which can be written in the matter basis as follows,

$$H = \begin{pmatrix} -\omega_m - A\cos(kr)\cos 2\theta_m & A\cos(kr)\sin 2\theta_m \\ A\cos(kr)\sin 2\theta_m & \omega_m + A\cos(kr)\cos 2\theta_m \end{pmatrix} \tag{8}$$

For a system for which the size of the perturbation, A, is smaller than the frequency of neutrino flavor oscillations corresponding to the constant matter density, ω_m, we can ignore the perturbation in the diagonal term. The off-diagonal term on the other hand can be rewritten using the trignometric identity,

$$\cos(kr) = \frac{e^{ikr} + e^{-ikr}}{2}. \tag{9}$$

The Hamiltonian for neutrinos propagating in medium with only one frequency on top of the constant matter density, is thus a combination of two terms of the form given in eq. **??**. One of the terms (e^{-ikr}) is very far away from resonance and we can ignore it. Ignoring this term can be justified by solving the full equations numerically and comparing it with the solution of eq. **??** which can be calculated analytically. Fig. **??** shows this comparison and an agreement to a very degree of accuracy.

In rest of the section we quantify what can be considered "on-resonance" and "off-resosnace". In the case of a single frequency profile, this is simpler than a general problem of a matter profile with several frequencies. However, the single frequency can help us gain an insight in to the general problem.

IV. INTERFERENCE OF RABI OSCILLATIONS AND MULTI-FREQUENCY MATTER PROFILE

The approach applied to single frequency matter profile also helps with the understanding of multi-frequency matter profile. However, multi-frequency matter profile leads to multiple modes of Rabi oscillations, even with our simplified approach by dropping the varying σ_3 term in Hamiltonian. In this section, we examine the interference between two modes of Rabi oscillations.

We explain the interference between different modes of Rabi oscillations using the idea of energy gap shift. Suppose we have a Rabi oscillation system with two modes, one mode at resonance with frequency $k_1 = \omega_{\rm m}$ and another mode with frequency k_2 that is off resonance. In some cases, there can be a significant transition amplitude decrease because of the off resonance frequency k_2, which can be interpreted as shift of energy gap due to the frequency k_2. To model the effect, we construct a Rabi oscillation Hamiltonian with two modes of different frequency,

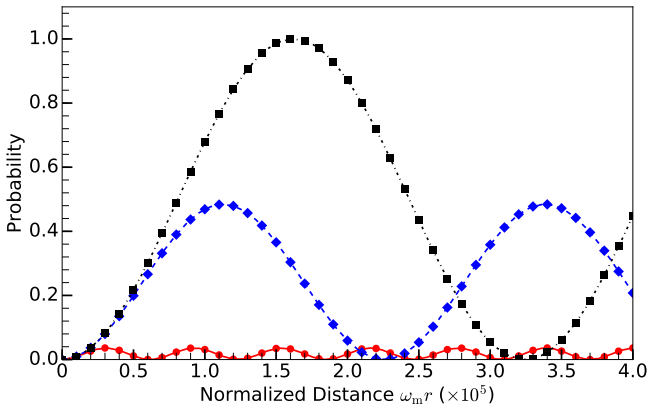

FIG. 1. Single frequency matter profile and Rabi oscillation. The markers are numerical results for the transition probabilities between two background mass eigenstates for the neutrinos with matter perturbation $A_1\sin(k_1 r)$. The dots, diamonds, and squares are for $k_1 = \omega_{\rm m}$, $k_1 = (1 - 2\times 10^{-5})\omega_{\rm m}$, and $k_1 = (1 - 10^{-4})\omega_{\rm m}$ respectively. The lines are the predictions using Rabi formula. During the calculation, λ_0 is set to 0.5 of the MSW resonance potential $\lambda_{\rm MSW} = \omega_{\rm v}\cos 2\theta_{\rm v}$ and mixing angle is chosen so that $\sin^2(2\theta_{\rm v}) = 0.093$.

$$H^{(\rm m)} = -\frac{\omega_{\rm m}}{2}\sigma_3 - \frac{1}{2}\sum_{n=1}^{N} A_n\cos(k_n r)\sigma_1 + \frac{1}{2}\sum_{n=1}^{N} A_n\sin(k_n r)\sigma_2, \tag{10}$$

where $N = 2$ for two frequency case. To show the destruction effect, the Hamiltonian Eq. (10) is reformed into a vector with sigma matrices $(\sigma_1, \sigma_2, \sigma_3)$ as the basis,

$$\mathbf{H} = \begin{pmatrix} 0 \\ 0 \\ \omega_m \end{pmatrix} + \begin{pmatrix} A_1\cos(k_1 r) \\ -A_1\sin(k_1 r) \\ 0 \end{pmatrix} + \begin{pmatrix} A_2\cos(k_2 r) \\ -A_2\sin(k_2 r) \\ 0 \end{pmatrix}. \tag{11}$$

The three terms are defined as $\mathbf{H}_3$, $\mathbf{H}_1$, and $\mathbf{H}_2$ respectively. $\mathbf{H}_1$ and $\mathbf{H}_2$ are two rotating vectors as a function of r with frequencies k_1 and k_2 in this vector space, while $\mathbf{H}_3$ is perpendicular to $\mathbf{H}_1$ and $\mathbf{H}_2$. To work out the energy gap shift, we go to the frame that corotates with $\mathbf{H}_2$, in which we have the new frequencies $k_1' = k_1 - k_2$ and $k_2' = 0$ as well as new energy gap $\omega_{\rm m}' = \omega_{\rm m} - k_2$. The resonance mode $\mathbf{H}_1$ retains on the resonance condition since $k_1' = \omega_{\rm m}'$, i.e. $k_1 - k_2 = \omega_{\rm m} - k_2$, holds in the new frame. On the other hand, we have two static fields $\mathbf{H}_3$ and $\mathbf{H}_2$ together as the new energy gap, as long as $\mathbf{H}_2 \ll \mathbf{H}_3$, which is the usual case. The new energy gap in this frame is calculated as

$$\begin{aligned}\tilde{\omega}_{\rm m}' =& {\rm sign}(\omega_{\rm m}')\sqrt{\omega_{\rm m}'^2 + A_2^2} \\ \approx& \omega_{\rm m}' + \frac{A_2^2}{2\omega_{\rm m}'} \\ =& \omega_{\rm m} - k_2 + \frac{1}{2}\frac{A_2^2}{\omega_{\rm m} - k_2}, \end{aligned} \tag{12}$$

where we kept only first order of Taylor series. The Taylor expansion in Eq. (12) holds as long as the relative detuning for the second frequency is large which means the second frequency is off resonance. As an approximation, the transitions between the two energy states follows the Rabi oscillations with energy gap $\tilde{\omega}_{\rm m}'$ and driving field with frequency $k_1' = k_1 - k_2$. Consequently, we can estimate how much the amplitude of the transition is suppressed due to k_1 mode by calculating the new relative detuning,

$$\begin{aligned} D' =& \frac{|k_1' - \tilde{\omega}_{\rm m}'|}{|A_1|} \\ =& \left| \frac{k_1 - \omega_{\rm m}}{A_1} + \frac{A_2^2}{2A_1(k_2 - \omega_{\rm m})} \right| \qquad (13) \\ =& \left| \frac{{\rm sign}(k_1 - \omega_{\rm m})}{{\rm sign}(k_2 - \omega_{\rm m})} D_1 + \frac{A_2}{2A_1 D_2} \right|, \qquad (14) \end{aligned}$$

where D_2 is the relative detuning of the second mode,

$$D_i = \left| \frac{k_i - \omega_{\rm m}}{A_i} \right|.$$

In principle, you can change the energy gap of the first frequency to approach the resonance or escape the resonance by carefully arranging the second frequency, which is also obvious from Eq. (14). However, for the purpose of the paper we only discuss the most important destruction effect by choosing $D_1 = 0$. We observe the importance of the relative detuning. For the second mode to significantly interfere with the first mode, we need a small D_2 and a large amplitude or width $A_2 \gg A_1$.

The condition can be verified by comparing the numerical solution and estimation using Rabi formula. However, we are most interested in the amplitude change due to $\mathbf{H}_2$ mode. Relative detuning is the only variable that we need to calculate the amplitude, hence we only compare the numerical results with estimated amplitudes using $1/(1 + D'^2)$. To verify the condition, we choose the first rotating perturbation to satisfy the resonance condition $k_1 = \omega_{\rm m}$, the condition for the second rotating field shifting the system out of resonance is that the relative detuning becomes larger than 1, which leads to

$$|A_2| \geq \sqrt{2\omega_{\rm m}|A_1(k_2 - \omega_{\rm m})|} \equiv A_{2,\rm Critical}. \tag{15}$$

We expect the transition amplitude to decrease as we have larger $|A_2|$.

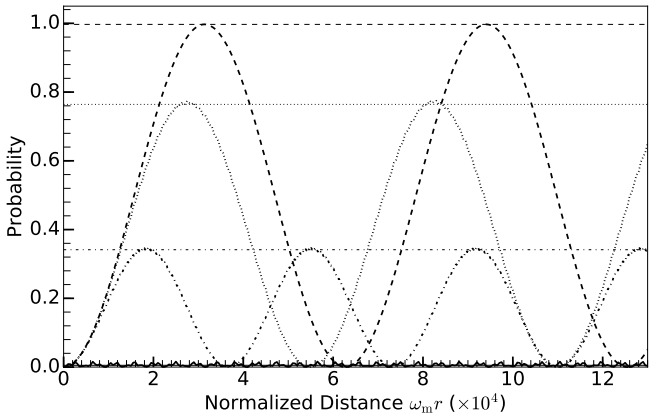

FIG. 2. Reduction of transition amplitudes due to interference. Dashed line, dotted line, dash-dotted line, and solid line are for $A_2 = 10^{-2}\omega_{\rm m}$, $k_2 = 10\omega_{\rm m}$, $A_2 = 10^{-2}\omega_{\rm m}$, $k_2 = 10^{-1}\omega_{\rm m}$, $A_2 = 5.0 \times 10^{-2}\omega_{\rm m}$, $k_2 = 10\omega_{\rm m}$, and $A_2 = 5 \times 10^{-2}\omega_{\rm m}$, $k_2 = 10^{-1}\omega_{\rm m}$. In all the calculations, we choose $A_1 = 10^{-4}\omega_{\rm m}$, $k_1 = \omega_{\rm m}$. The grid lines are the transition amplitudes estimated using D'. During the calculation, Λ_0 is set to half of the MSW resonance potential, $\Lambda_0 = \frac{1}{2}\lambda_{\rm MSW} = \frac{1}{2}\omega_{\rm v}\cos 2\theta_{\rm v}$.

We choose the two modes where the first one has amplitude $A_1 = 10^{-4}\omega_{\rm m}$ and frequency $k_1 = \omega_{\rm m}$. With a small amplitude of the second frequency, $A_2 = 10^{-4}\omega_{\rm m}$, and large frequency $k_2 = 10\omega_{\rm m}$, we obtain almost full resonance. For larger A_2 the destruction effect is more effective, as shown in Fig. 2. The estimations of transition amplitude are in good agreement with the numerical results. To show the importance of relative detuning, we calculated the relative detuning for each cases, which are 0.06, 0.6, 1.4, 13.9 for the lines from top to down. We also notice that the width of each cases doesn't change since we kept A_1 fixed for each calculation, which indicates that the decreasing in transition amplitude is because of the increasing in detuning.

Even for the single frequency matter profile, there are two modes of Rabi oscillations $\pm k_1$, under the approximation that the varying σ_3 term in Hamiltonian is neglected, as mentioned in Sec. III. The three examples calculated in Fig. 1 are almost exact since the modification of relative detuning for the k_1 mode that we kept, due to the far off resonance mode $-k_1$ that we neglected, is tiny. The first two lines of Table. I show the relative detunings of the three cases in Fig. 1, where $n = \pm 1$ are for the $\pm k_1$ modes in the Hamiltonian **??**. We observe in Fig. 1 that the relative detuning change due to an extra

$-k_1$ mode is not observable.

V. PARAMETRIC RESONANCE AND RABI OSCILLATION — JACOBI-ANGER EXPANSION

With the intuition of the Rabi oscillations itself as well as the interference between different modes of Rabi oscillations shown in Sec. IV, we expect to interpret the transition probabilities of any matter profile more precisely if the system can be exactly decomposed into multiple Rabi oscillations. Kneller et. al provided a method to achieve this goal [11], namely the Jacobi-Anger expansion. In this section, we show that the matter effect can be decomposed into superpositions of Rabi oscillations by applying a Jacobi-Anger expansion to the Hamiltonian. Our approach is to apply a designed unitary transformation first which make the motivation of Jacobi-Anger expansion, before writing down the final result as superpositions of Rabi oscillation using Jacobi-Anger expansion. For a system with general matter perturbation, c.f. Eq. (**??**), we apply an unitary transformation of the form

$$\mathbf{U} = \begin{pmatrix} e^{-\mathrm{i}\eta(r)} & 0 \\ 0 & e^{\mathrm{i}\eta(r)} \end{pmatrix}, \tag{16}$$

which is a transformation used in Ref. 13 to remove the diagonal elements of the Hamiltonian. This transformation is essentially a rotation $\exp\left(-\mathrm{i}\frac{\sigma_3}{2}\cdot 2\eta\right)$. In this work, this transformation is used to remove the varying σ_3 terms $\delta\lambda(r)\cos 2\theta_\mathrm{m}\sigma_3/2$ in the Hamiltonian, so that the energy gap is fixed in the new basis $\left(|\nu_\mathrm{r1}\rangle, |\nu_\mathrm{r2}\rangle\right)^\mathrm{T}$, which is defined as

$$\begin{pmatrix} |\nu_\mathrm{r1}\rangle \\ |\nu_\mathrm{r2}\rangle \end{pmatrix} = \mathbf{U}^\dagger \begin{pmatrix} |\nu_\mathrm{L}\rangle \\ |\nu_\mathrm{H}\rangle \end{pmatrix}. \tag{17}$$

For convenience, we name this unitary transformation in Eq. (16) Rabi transformation as well as the new basis in Eq. (17) the Rabi basis. The reason it can remove the σ_3 term is that it will transform the system into a rotating frame so that the varying energy gap due to the fluctuating matter density is exactly canceled by rotation of the frame. In Rabi basis, we find the Schrödinger equation

$$\begin{pmatrix} \frac{\mathrm{d}\eta}{\mathrm{d}r} & 0 \\ 0 & -\frac{\mathrm{d}\eta}{\mathrm{d}r} \end{pmatrix} \begin{pmatrix} \psi_\mathrm{R1} \\ \psi_\mathrm{R2} \end{pmatrix} + \mathrm{i}\frac{\mathrm{d}}{\mathrm{d}r}\begin{pmatrix} \psi_\mathrm{R1} \\ \psi_\mathrm{R2} \end{pmatrix} = \left[-\frac{\omega_\mathrm{m}}{2}\sigma_3 + \frac{\delta\lambda}{2}\cos 2\theta_\mathrm{m}\sigma_3 - \frac{\delta\lambda}{2}\sin 2\theta_\mathrm{m}\begin{pmatrix} 0 & e^{2\mathrm{i}\eta} \\ e^{-2\mathrm{i}\eta} & 0 \end{pmatrix}\right]\begin{pmatrix} \psi_\mathrm{R1} \\ \psi_\mathrm{R2} \end{pmatrix},$$

in which the varying diagonal elements in Hamiltonian can be eliminated by choosing $\eta(r)$ properly, i.e.,

$$\eta(r) - \eta(0) = \frac{\cos 2\theta_\mathrm{m}}{2}\int_0^r \delta\lambda(\tau)d\tau. \tag{18}$$

In Rabi basis, the Schrödinger equation becomes

$$\mathrm{i}\frac{d}{dr}\begin{pmatrix} \psi_\mathrm{r1} \\ \psi_\mathrm{r2} \end{pmatrix} = \left[-\frac{\omega_\mathrm{m}}{2}\sigma_3 - \frac{\delta\lambda}{2}\sin 2\theta_\mathrm{m}\begin{pmatrix} 0 & e^{2\mathrm{i}\eta} \\ e^{-2\mathrm{i}\eta} & 0 \end{pmatrix}\right]\begin{pmatrix} \psi_\mathrm{r1} \\ \psi_\mathrm{r2} \end{pmatrix}.$$

One can easily show that the transition probability between two eigenstates in Rabi basis is the same as the transition probability between two eigenstates in background matter basis, given the initial condition that the system is in low energy state.

For single frequency matter profile with potential $\delta\lambda(r) = A_1\sin(k_1 r)$, we have $\eta(r) = -A_1\cos 2\theta_\mathrm{m}\cos(k_1 r)/(2k)$. To make connection with Rabi oscillation, we apply Jacobi-Anger expansion, which is used in Ref. 11, to decompose the $\exp\left(\mathrm{i}z\cos\left(k_1 r\right)\right)$-like term in Hamiltonian into linear combinations of terms that is proportional to $\exp\left(\mathrm{i}nk_1 r\right)$, i.e., to decompose spherical waves into plane waves. The decomposed form of Hamiltonian explicitly shows that the Hamiltonian is a summation of Rabi systems, which is

$$H^{(\mathrm{R})} = -\frac{\omega_\mathrm{m}}{2} - \frac{1}{2}\sum_{n=-\infty}^{\infty} B_n \begin{pmatrix} 0 & \Phi_n e^{\mathrm{i}nk_1 r} \\ \Phi_n^* e^{-\mathrm{i}nk_1 r} & 0 \end{pmatrix},$$

where

$$B_n = \tan 2\theta_\mathrm{m} n k_1 J_n\left(\frac{A_1}{k_1}\cos 2\theta_\mathrm{m}\right),$$
$$\Phi_n = e^{i\pi(3n/2+1)},$$

with J_n standing for the Bessel function. The constant phase Φ_n doesn't play any role for the reason discussed in Appendix A. Phase in matter potential would also go into Φ_n, for which reason, phase of matter profile is not included in the current discussion. In the Hamiltonian, the first term describes the energy gap, while the second term is the summation of many driving fields. The resonance width for a given mode n is $|B_n|$. It's worth mentioning that we have [14]

$$J_n(n\operatorname{sech}\alpha) \sim \frac{e^{n(\tanh\alpha-\alpha)}}{\sqrt{2\pi n\tanh\alpha}} \tag{19}$$

for large n. It's straightforward to prove that resonance width decreases dramatically for large n thus resonance of higher order modes become insignificant.

When the system has one dominate resonance mode and without significant interference between the resonance mode and other modes, all off-resonance modes can be dropped without significantly changing the transition probabilities. However, as we have shown previously in Sec. IV, interference might happen between different modes and interferences were measured with a criteria. However, interference is not the only effect we need to consider. The following subsections will determine the important modes of the system (i.e., which n to include) and explore the interference between modes hence explain the coincidence presented in the previous sections. We use dimensionless quantities which are scaled using the characteristic energy scale $\omega_{\rm m}$, e.g.,

$$\begin{aligned}\hat{r} &= \omega_{\rm m} r,\\ \hat{k}_1 &= \frac{k_1}{\omega_{\rm m}},\\ \hat{A}_1 &= \frac{A_1}{\omega_{\rm m}},\\ \hat{B}_n &= \frac{B_n}{\omega_{\rm m}}.\end{aligned}$$

A. The Important Factors

In order for a mode to have a significant effect on the transition probabilities, we require it to has large relative detuning D, and a large oscillation wavelength compared to the size of the physical system. Relative detuning for each mode is calculated as

$$D_n = \frac{|nk_1 - \omega_{\rm m}|}{B_n} \tag{20}$$

for single frequency matter profile, and

$$D_{\{n_a\}} = \frac{|\sum_a n_a k_a - \omega_{\rm m}|}{B_{\{n_a\}}} \tag{21}$$

for multi-frequency matter profile.

For modes with small relative detuning, they are important since they might lead to full transition. However, the full transition requires at least a distance of the order of the wavelength of the oscillation. Suppose we have a mode that has zero relative detuning, but with a oscillation wavelength much larger than the size of the system, such a mode would never have the chance to accumulate a large transition probability within the size of the system. By utilizing the theory of Rabi oscillation, we know that the oscillation wavelength of each mode is determined by the Rabi frequency

$$\Omega_{\{n_a\}} = |B_{\{n_a\}}|\sqrt{1 + D^2_{\{n_a\}}}. \tag{22}$$

Thus modes that has much larger oscillation wavelength are not subjected to be considered even though their relative detunings are close to zero.

In principle, we can always approximate the system by including more modes with larger relative detuning while neglecting the modes with wavelength much longer than the size of physical system. However such effort doesn't simplify the calculations.

B. Single Frequency Matter Profile Revisited

For the single frequency matter potential $\lambda = \lambda_0 + \lambda_1 \sin(k_1 r)$ discussed in Sec. III, we removed the varying σ_3 term by arguing that this term has no effect on transition probabilities when the system is close to resonance, $k_1 \sim \omega_{\rm m}$. The reason is that only the first mode $n = 1$ is on resonance when $k_1 = \omega_{\rm m}$ and all other modes are far from resonance, thus

$$\begin{aligned}H^{\rm R} &\approx -\frac{\omega_{\rm m}}{2}\sigma_3 - \frac{1}{2}B_1 \begin{pmatrix} 0 & \Phi_1 e^{ik_1 r} \\ \Phi_1^* e^{-ik_1 r} & 0 \end{pmatrix} \\ &\approx -\frac{\omega_{\rm m}}{2}\sigma_3 - \frac{A_1}{2}\cos(k_1 r)\sigma_1 + \frac{A_1}{2}\sin(k_1 r)\sigma_2,\end{aligned} \tag{23}$$

where A_1 is defined in Eq. (**??**) and approximation

$$J_1\left(\frac{\lambda_1}{k_1}\cos(2\theta_{\rm m})\right) \approx \frac{\lambda_1}{2k_1}\cos(2\theta_{\rm m})$$

for $\lambda_1 \cos(2\theta_{\rm m})/k_1 \ll 1$ is used in the last step. Thus we reach a similar equation to the approximation we used in Sec. III. $\lambda_1 \cos(2\theta_{\rm m})/k_1 \ll 1$ corresponds to small resonance width for Eq. (**??**) and also Eq. (23) so that the interferences are small.

Using Jacobi-Anger expansion, we can calculate the relative detuning for each mode as well as the interference effect. The relative detuning for each mode in the Jacobi-Anger expansion for single frequency matter profile used in Fig. 1 is calculated and listed in Table. I. The D_1' is the shifted relative detuning of the first mode with $n = 1$ due to other mode. It clearly shows that the first mode takes the whole system so that the approximation of neglecting the varying σ_3 terms in Hamiltonian is accurate enough. One can also show that the interference effect due to higher order modes is negligible, since they do not change the relative detuning of the most significant modes.

C. Castle Wall Matter Profile

For completeness of this paper, we show one example of multi-frequency matter profile. One of the multi-frequency matter profiles that has been well studied is the castle wall matter profile. Using Fourier series, any matter profile can be Fourier decomposed into superposition of many single frequency matter profile in principle. We decompose the periodic castle wall matter profile into many frequencies and study the interference effect. The potential shown in Fig. 3 is defined as,

$$\lambda(r) = \begin{cases} \Lambda_1, & -\frac{X_1}{2} + nX \le r \le \frac{X_1}{2} + nX \\ \Lambda_2, & \frac{X_1}{2} + nX \le r \le \frac{X_1}{2} + \frac{X_2}{2} + nX \end{cases} \tag{24}$$

TABLE I. Relative detuning and oscillation wavelength of each mode for single frequency matter profile.

$k_1 = \omega_{\rm m}$				$k_1 = (1-2\times10^{-5})\omega_{\rm m}$				$k_1 = (1-10^{-4})\omega_{\rm m}$			
n	D	D_1'	$2\pi\omega_{\rm m}/\Omega_n$	n	D	D_1'	$2\pi\omega_{\rm m}/\Omega_n$	n	D	D_1'	$2\pi\omega_{\rm m}/\Omega_n$
1	0	-	3.2×10^5	1	1	-	2.2×10^5	1	5.2	-	6.2×10^4
-1	10^5	4.8×10^{-6}	3.1	-1	10^5	1	3.1	-1	10^5	5.2	3.1
2	1.1×10^9	2.1×10^{-14}	6.3	2	1.1×10^9	1	6.3	2	1.1×10^9	5.2	6.3
-2	3.4×10^9	6.9×10^{-15}	2.1	-2	3.4×10^9	1	2.1	-2	3.4×10^9	5.2	2.1

where X_1 and X_2 are the two periods of the matter profile or potential, $X = X_1 + X_2$, and n is integer. The parametric resonance condition derived by E. Akhmedov [5] is,

$$\frac{\tan(\omega_{\rm m1}X_1/2)}{\tan(\omega_{\rm m2}X_2/2)} = -\frac{\cos 2\theta_{\rm m2}}{\cos 2\theta_{\rm m1}}, \tag{25}$$

where $\omega_{{\rm m}i}$ and $\theta_{{\rm m}i}$ are the energy difference and mixing angle for potential Λ_1 and Λ_2 respectively.

Even though this castle wall problem is analytically solved, the resonance condition Eq. (25) itself is not transparent. In this subsection, we show that such a system is closed related to Rabi oscillations. For illustration purpose, we set the profile to be equal period for the two densities so that $X_1 = X_2 \equiv X/2$. To show that the neutrino flavor conversions in this castle wall matter profiles is related to Rabi oscillation, we decompose the profile using Fourier series,

$$\lambda(r) = \lambda_0 + \sum_{n=1}^{\infty} \lambda_n \cos\left(k_n r\right), \tag{26}$$

where

$$\begin{aligned}
\lambda_0 &= (\Lambda_1 + \Lambda_2)/2, \\
\lambda_n &= \frac{2}{(2n-1)\pi}(-1)^n\left(\Lambda_1 - \Lambda_2\right), \\
k_n &= (2n-1)k_0, \\
k_0 &= 2\pi/X.
\end{aligned}$$

To calculate the transitions between two mass states of background matter potential λ_0, we use the background matter basis with respect to λ_0, in which the transition is zero when varying matter profile vanishes. The Hamiltonian

$$H^{(\rm m)} = -\frac{1}{2}\omega_{\rm m}\sigma_3 + \frac{1}{2}\sum_{n=1}^{\infty}\lambda_n \cos 2\theta_{\rm m}\cos\left(k_n r\right)\sigma_3 - \frac{1}{2}\sum_{n=1}^{\infty}\lambda_n \sin 2\theta_{\rm m}\cos\left(k_n r\right)\sigma_1, \tag{27}$$

determines the transitions between the two background matter states.

In principle, the base frequency k_0 which is determined by the total period X can be arbitrary. In this example, we choose a X so that the base frequency k_0 matches the energy gap $\omega_{\rm m}$. Even though multiple perturbation frequencies show up in Eq. (27), we identify that only the first frequency $n = 1$ is the resonance frequency since we are using $k_0 = \omega_{\rm m}$. As an approximation, we drop all other frequencies $n > 2$ regarding the fact that they are far from resonance. Thus, similar to single frequency matter profile, the varying σ_3 terms have limited effects on the transition probabilities in our case, which leads to

$$\begin{aligned}
H^{(\rm m)} &\to -\frac{1}{2}\omega_{\rm m}\sigma_3 - \frac{1}{2}\sum_{n=1}^{2}\lambda_n \sin 2\theta_{\rm m}\cos\left(k_n r\right)\sigma_1 \\
&\to -\frac{1}{2}\omega_{\rm m}\sigma_3 - \frac{1}{2}\sum_{n=1}^{2}A_n\cos(k_n r)\sigma_1 \\
&\quad + \frac{1}{2}\sum_{n=1}^{2}A_n\sin(k_n r)\sigma_2,
\end{aligned}$$

where

$$A_n = \frac{\lambda_n \sin 2\theta_{\rm m}}{2}.$$

The relative detuning is 0 if we have only the first mode. However, it becomes

$$D_1' = \frac{A_2^2}{2|A_1(\omega_{\rm m} - k_2)|}, \tag{28}$$

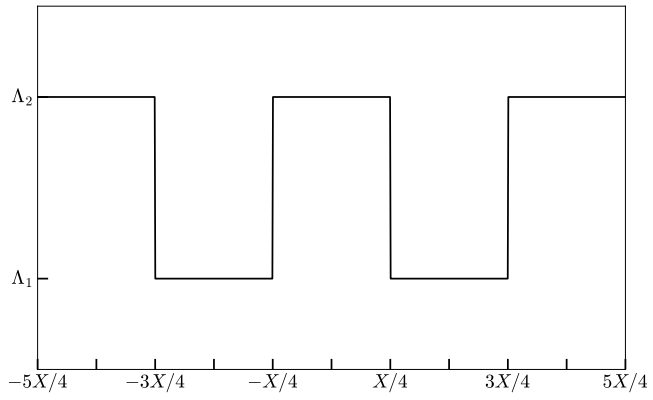

FIG. 3. The castle wall matter potential profile with $X_1 = X_2 = X/2$.

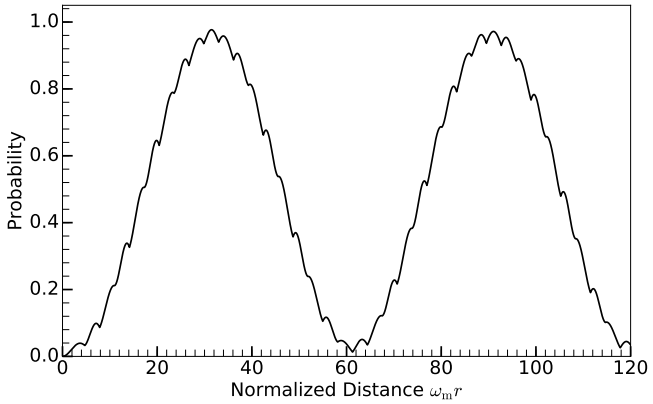

FIG. 4. Transition probabilities for castle wall matter profile calculated numerically for $\Lambda_2 - \Lambda_1 = 0.4\Lambda_0$. During the calculation, the energy of neutrinos is 10 MeV, mass-squared difference is $\delta m^2 = 2.6 \times 10^{-3}\,\mathrm{eV}^2$, and the vacuum mixing angle chosen so that $\sin^2(2\theta_v) = 0.093$. The background potential Λ_0 is chosen so that it's half the MSW resonance potential, $\Lambda_0 = \frac{1}{2}\lambda_{\mathrm{MSW}} = \frac{1}{2}\omega_{\mathrm{v}} \cos 2\theta_{\mathrm{v}}$, and the base frequency is set to $k_0 = 2\pi/X = \omega_{\mathrm{m}}$.

if we include the second frequency k_2. One feature of this Fourier series expanded matter profile Eq. (26) is that the width of each frequency decreases as the order n increases while the detuning of each frequency increases. We calculate the relative detuning for each frequency

$$D_n = \frac{|k_n - \omega_{\mathrm{m}}|}{|\lambda_n \sin 2\theta_{\mathrm{m}}/2|} = \frac{2(n-1)(2n-1)\pi\omega_{\mathrm{m}}}{(\Lambda_2 - \Lambda_1)\sin 2\theta_{\mathrm{m}}} \qquad (29)$$

which is quadratic in n and inversely proportional to $\Lambda_2 - \Lambda_1$. We find that all higher frequencies k_n for $n > 2$ have very large relative detunings. The neutrino transition probability between the two matter states is shown in FIG. 4, where we find the system has almost full transition.

A more rigorous treatment is to use Jacobi-Anger expansion and find the Rabi modes, where we find that the mode that corresponds to single frequency k_1 dominates and all other modes have little destruction effect on it. Quantitatively, higher orders leads to smaller width $B_{\{n_i\}}$ yet larger detuning $\sum_n nk_n - \omega_{\mathrm{m}}$, which renders a smaller effect on the resonance mode $\{1, 0\}$, since the effect is evaluated as Eq. (14). Table II lists the first few smallest relative detunings of Fig. 4. The second column is the relative detuning of the corresponding mode, while the third column is the relative detuning of mode $\{1, 0\}$ with the energy gap shift effect of the corresponding mode.

TABLE II. Relative detuning of each frequency.

$\{n_1, n_2\}$	D	$D'_{\{1,0\}}$
$\{1, 0\}$	0	-
$\{-1, 0\}$	48	1.0×10^{-2}
$\{0, 1\}$	1.5×10^2	1.1×10^{-3}
$\{2, 0\}$	2.4×10^2	2.0×10^{-4}

VI. CONCLUSIONS

In conclusion, we have provided an interpretation for neutrino flavor conversion in fluctuating matter with the help of Rabi oscillations. The work provided two different points of view that is related to Rabi oscillations.

The first point of view was to interpret the neutrino flavor conversions in background matter basis. In this basis, matter density fluctuations will introduced a fluctuation part to the diagonal elements of the Hamiltonian, which means that the energy gap is fluctuating if we draw analogy between this Hamiltonian and the Hamiltonian of Rabi oscillations. For neutrino flavor conversions in a single frequency matter profile, the neutrino flavor oscillations becomes large when the matter fluctuation frequency is close to the energy gap, which is the resonance condition. We anticipated that the fluctuations of energy gap have limited effects on neutrino flavor conversions under this resonance condition. Thus the matter fluctuation only works as a pure flipping field that converts neutrinos from one flavor to another.

As we added more frequencies of matter density fluctuations, the neutrino flavor conversions becomes nontrivial due to the interferences between the difference matter profile frequencies. To quantify the interference between different Rabi oscillation modes, we defined relative detuning which describes how off-resonance a Rabi oscillation is. In the case of single frequency Rabi oscillations, the relative detuning becomes 0 under the resonance condition. As a second frequency is added to the oscillations, the energy gap is shifted due to this new frequency. A measure of the interference effect is to consider the relative detuning of the first frequency which is at resonance, under the shifted energy gap. Numerical results verified this conjecture. With the interference mechanism, we revisit the single frequency matter profile neutrino oscil-

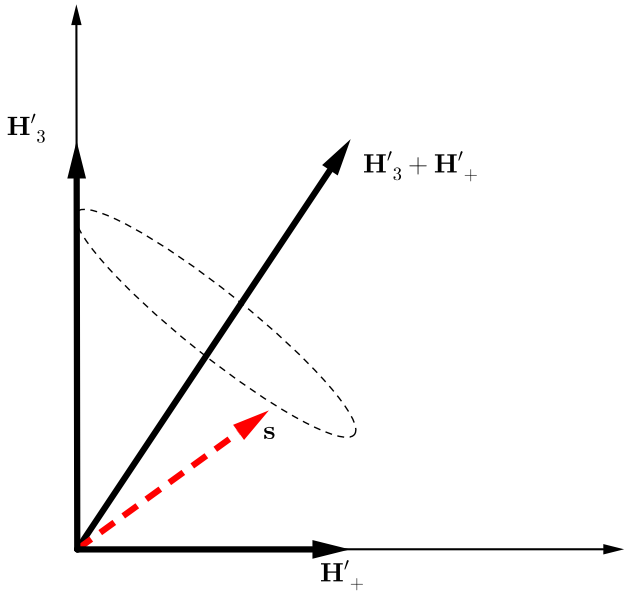

FIG. 5. Rabi oscillations in corotating frame. The red dashed vector is the flavor isospin, while the black solid vectors are the vectors of Hamiltonian. The flavor isospin vector is precessing around vector of total Hamiltonian $\mathbf{H}_3 + \mathbf{H}_+$.

lations.

Another view is to switch to a basis where the neutrino oscillations Hamiltonian is decomposed into infinite Rabi oscillations. Equivalently speaking, the oscillations are consequences of superposition of Rabi oscillations, which we call modes of oscillations. This view was applied to emphasis the approximations that the change of energy gap due to matter fluctuation can be neglected under resonance condition in the previous background matter basis.

VII. ACKNOWLEDGEMENT

The first author would like to thank J. Kneller and K. Patton for their help during this research. This research is supported by DOE EPSCoR grant #DE-SC0008142.

Appendix A: Rabi Oscillations

In this appendix we introduce flavor isospin [15] to Rabi oscillations and derive the transition probabilities as well as explain the resonance and width briefly.

The Hamiltonian for Rabi oscillation is

$$H_{\rm R} = -\frac{\omega_{\rm R}}{2}\sigma_3 - \frac{A_{\rm R}}{2}\left(\cos(k_{\rm R}t+\phi_{\rm R})\sigma_1 - \sin(k_{\rm R}t+\phi_{\rm R})\sigma_2\right), \tag{A1}$$

in which $\omega_{\rm R}$ serves as the energy split of the two level system, while $A_{\rm R}$ and $k_{\rm R}$ are the strength and frequency of the driving field, respectively. A decomposition of the second term shows that

$$H_{\rm R} = -\frac{\boldsymbol{\sigma}}{2}\cdot(\mathbf{H}_3 + \mathbf{H}_+),$$

where $\boldsymbol{\sigma}$ is the the vector of Pauli matrices, and the three vectors are

$$\mathbf{H}_3 = \begin{pmatrix} 0 \\ 0 \\ \omega_{\rm R} \end{pmatrix}, \tag{A2}$$

$$\mathbf{H}_+ = \begin{pmatrix} A_{\rm R}\cos(k_{\rm R}t+\phi_{\rm R}) \\ -A_{\rm R}\sin(k_{\rm R}t+\phi_{\rm R}) \\ 0 \end{pmatrix}. \tag{A3}$$

The three vectors are mapped onto a Cartesian coordinate system, so that $\mathbf{H}_3$ is the vector aligned with the third axis, $\mathbf{H}_+$ is a rotating vectors in a plane perpendicular to $\mathbf{H}_3$. The wave function $\Psi = (\psi_1, \psi_2)^{\rm T}$ is also used to define the state vector $\mathbf{s}$

$$\mathbf{s} = \Psi^\dagger \frac{\boldsymbol{\sigma}}{2}\Psi \tag{A4}$$

$$= \frac{1}{2}\begin{pmatrix} 2\,{\rm Re}\,(\psi_1^*\psi_2) \\ 2\,{\rm Im}\,(\psi_1^*\psi_2) \\ |\psi_1|^2 - |\psi_2|^2 \end{pmatrix} \tag{A5}$$

The third component of $\mathbf{s}$, which is denoted as s_3, is within range $[-1/2, 1/2]$. The two limits, $s_3 = -1/2$ and $s_3 = 1/2$ stand for the system in high energy state and low energy state respectively. $s_3 = 0$ if the system has equal probabilities to be on high energy state and low energy state. The Schrödinger equation becomes

$$\frac{\rm d}{{\rm d}t}\mathbf{s} = \mathbf{s}\times\mathbf{H}, \tag{A6}$$

which is the precession equation. For static $\mathbf{H}$, the state vector $\mathbf{s}$ precess around $\mathbf{H}$.

In a frame that corotates with $\mathbf{H}_+$, which is described in Fig. 5, the new Hamiltonian is

$$\frac{\rm d}{{\rm d}t}\mathbf{s} = \mathbf{s}\times(\mathbf{H}'_3 + \mathbf{H}_+), \tag{A7}$$

where

$$\mathbf{H}'_3 = \begin{pmatrix} 0 \\ 0 \\ \omega_{\rm R} - k_{\rm R} \end{pmatrix}, \qquad \mathbf{H}'_+ = \begin{pmatrix} A_{\rm R} \\ 0 \\ 0 \end{pmatrix}. \tag{A8}$$

The state vector $\mathbf{s}$ precess around a static vector $\mathbf{H}'_3 + \mathbf{H}'_+$ with a frequency $\Omega_{\rm R} = \sqrt{|A_{\rm R}|^2 + (k_{\rm R}-\omega_{\rm R})^2}$. A geometric analysis by projecting the state vector $\mathbf{s}$ on to the verticle axis shows that

$$s_3 = \frac{1}{2} - \frac{|A_{\rm R}|^2}{\Omega_{\rm R}^2}\sin^2\left(\frac{\Omega_{\rm R}}{2}t\right). \tag{A9}$$

Resonance occurs when the term $\mathbf{H}_3$ disappears in this corotating frame, since the state vector $\mathbf{s}$ converts completely between $+1/2$ (low energy state) and $-1/2$ (high energy state).

Such a system has analytical transition probability from low energy state to high energy state

$$P(t) = \frac{1}{2}(1 - 2s_3(t)) = \frac{|A_{\rm R}|^2}{\Omega_{\rm R}^2} \sin^2\left(\frac{\Omega_{\rm R}}{2}t\right), \quad \text{(A10)}$$

where

$$\Omega_{\rm R} = \sqrt{|A_{\rm R}|^2 + (k_{\rm R} - \omega_{\rm R})^2} \quad \text{(A11)}$$

is known as Rabi frequency. The detuning, which is defined by $k_{\rm R} - \omega_{\rm R}$, determines how off-resonance the system is, and amplitude of driving field $A_{\rm R}$ determines the resonance width,

$$\text{Detuning} = |k_{\rm R} - \omega_{\rm R}|, \quad \text{(A12)}$$
$$\text{Resonance Width} = |A_{\rm R}|. \quad \text{(A13)}$$

The transition probability oscillates with frequency $\Omega_{\rm R}$. However, the amplitude A_1 is the dominate factor for oscillation frequency when the system is close to resonance. The phase of the matter potential $\phi_{\rm R}$ has no effect on the transition probability since it only determines the initial phase of driving Hamiltonian vector $\mathbf{H}_+$. We also notice that the transition amplitude is determined by relative detuning D, which is defined as

$$D = \left|\frac{k_{\rm R} - \omega_{\rm R}}{A_{\rm R}}\right|. \quad \text{(A14)}$$

Given a Rabi oscillation system with two driving frequencies

$$H_{\rm R} = -\frac{\omega_{\rm R}}{2}\sigma_3 - \frac{A_1}{2}\left(\cos(k_1 t + \phi_1)\sigma_1 - \sin(k_1 t + \phi_1)\sigma_2\right) - \frac{A_2}{2}\left(\cos(k_2 t + \phi_2)\sigma_1 - \sin(k_2 t + \phi_2)\sigma_2\right)$$

we decompose it into $\mathbf{H}_{\rm R} = \mathbf{H}_3 + \mathbf{H}_1 + \mathbf{H}_2$, where

$$\mathbf{H}_1 = \begin{pmatrix} A_1\cos(k_1 t + \phi_1) \\ A_1\sin(k_1 t + \phi_1) \\ 0 \end{pmatrix}, \mathbf{H}_2 = \begin{pmatrix} A_2\cos(k_2 t + \phi_2) \\ A_2\sin(k_2 t + \phi_2) \\ 0 \end{pmatrix}.$$

Assume $\mathbf{H}_1$ is the on-resonance perturbation which requires $k_1 = \omega_{\rm R}$. The most general condition that we can drop the new perturbation $\mathbf{H}_2$ is to make sure k_2 is far from the resonance condition compared to the resonance width,

$$D \equiv \frac{|k_2 - \omega_{\rm R}|}{|A_2|} \gg 1. \quad \text{(A15)}$$

The transition amplitude between the two states becomes

$$P(t) = \frac{1}{1 + D^2}\sin^2(\frac{\Omega_{\rm R}}{2}t). \quad \text{(A16)}$$

[1] S. P. Mikheev and A. Yu. Smirnov, Sov. J. Nucl. Phys. **42**, 913 (1985), [Yad. Fiz.42,1441(1985)].
[2] L. Wolfenstein, Physical Review D **17**, 2369 (1978).
[3] L. Wolfenstein, Physical Review D **20**, 2634 (1979).
[4] P. Krastev and A. Smirnov, Physics Letters B **226**, 341 (1989).
[5] E. K. Akhmedov, Pramana **54**, 47 (2000), arXiv:9907435 [hep-ph].
[6] B. Muller and H.-T. Janka, Monthly Notices of the Royal Astronomical Society **448**, 2141 (2015).
[7] S. M. Couch and C. D. Ott, The Astrophysical Journal **799**, 5 (2015).
[8] F. N. Loreti and A. B. Balantekin, Physical Review D **50**, 4762 (1994), arXiv:9406003 [nucl-th].
[9] A. Friedland and A. Gruzinov, "Neutrino signatures of supernova turbulence," (2006), arXiv:0607244 [astro-ph].
[10] J. Kneller and C. Volpe, Physical Review D **82**, 123004 (2010), arXiv:1006.0913.
[11] J. P. Kneller, G. C. McLaughlin, and K. M. Patton, Journal of Physics G: Nuclear and Particle Physics **40**, 055002 (2013), arXiv:arXiv:1202.0776v1.
[12] K. M. Patton, J. P. Kneller, and G. C. McLaughlin, Physical Review D **89**, 073022 (2014), arXiv:arXiv:1407.7835v1.
[13] J. P. Kneller and G. C. McLaughlin, Physical Review D **73**, 056003 (2006).
[14] I. Ploumistakis, S. Moustaizis, and I. Tsohantjis, Physics Letters A **373**, 2897 (2009).
[15] H. Duan, G. M. Fuller, and Y.-Z. Qian, Physical Review D **74**, 123004 (2006), arXiv:0703776 [astro-ph].